Isothermal Elimination of *n*-Alkylsulfinyl OC_1C_{10}-PPV Precursor Polymers Studied with FT-IR, UV−Vis, and MTDSC: Kinetics of the Elimination Reaction

E. Kesters,[†] S. Swier,[‡] G. Van Assche,[‡] L. Lutsen,[§] D. Vanderzande,[†,§] and B. Van Mele*[,‡]

IMO, Division Chemistry, Universiteit Hasselt, Campus Diepenbeek, Agoralaan Bld. D, 3590 Diepenbeek, Belgium; Department of Physical Chemistry and Polymer Science, Vrije Universiteit Brussel (VUB), Pleinlaan 2, 1050 Brussel, Belgium; and Division IMOMEC, IMEC, Wetenschapspark 1, 3590 Diepenbeek, Belgium

Received August 3, 2005; Revised Manuscript Received February 25, 2006

ABSTRACT: The conversion of *n*-alkylsulfinyl OC_1C_{10}-PPV precursor polymers to the conjugated OC_1C_{10}-PPV polymer and the subsequent reactions of the elimination products in the solid state are studied in situ with FT-IR, UV−vis spectroscopy, and modulated temperature DSC (MTDSC). FT-IR and UV−vis spectroscopy allow monitoring the formation of double bonds in the conjugated system. The experimental activation energy of this conversion reaction is in good agreement with the value from theoretical modeling (101 kJ/mol). Quasi-isothermal MTDSC heat capacity measurements permit the characterization of the subsequent reaction steps of the elimination products (dimerization of sulfenic acid and disproportionation of thiosulfinate). The formation of water in the dimerization step and elimination products results in a positive reaction heat capacity ($\Delta_r C_p$). This increase in heat capacity is slower than the formation of double bonds, which is attributed to the fact that the dimerization and disproportionation reactions behave as consecutive reactions relative to the elimination reaction of sulfenic acid. The amount of water released in isothermal conditions can be calculated from subsequent nonisothermal MTDSC experiments and can be used as an independent measure for the extent of the dimerization reaction. Isothermal and nonisothermal MTDSC experiments in solution have shown that phase separation between the polymer and the solvent occurs. In the nonisothermal experiment a small baseline shift is visible in the heat capacity signal at high temperature, which is an indication of phase separation. In the isothermal experiments, the increase in heat capacity is larger for the elimination in solution compared to the elimination in solid state, which is also an indication not only that the increase in heat capacity is due to the elimination process itself but also that phase separation interferes beyond a certain conversion. Phase separation in isothermal conditions is also demonstrated with UV−vis spectroscopy.

Introduction

The microstructure of conjugated polymers is of major importance for their performance in applications; e.g., quality and morphology of the conjugated system strongly affect the performance of the material in light-emitting diodes (LEDs). In the case of precursor systems, these properties may be strongly influenced by the elimination reaction. A large number of papers deal with the conversion of sulfonium poly(*p*-phenylenevinylene) (PPV) precursor polymers.[1] The broad range of elimination conditions that are defined in these reports, however, underlines the difficulty of monitoring the conversion reaction. For the sulfinyl-PPV precursor polymers, the elimination was performed at 280 °C based on thermogravimetric analysis (TGA) because other tools for studying the elimination reaction were not available at that time.[2] Some years later, de Kok et al. investigated the conversion process in more detail by means of ex-situ heating experiments.[3,4] A lot of questions, however, remained unanswered. To monitor the elimination reaction of sulfinyl-PPV precursor polymers toward conjugated polymers, several complementary in-situ analytical techniques are needed. In a previous paper, FT-IR spectroscopy, UV−vis spectroscopy, and TGA in nonisothermal mode were employed to gain a first insight into the elimination and degradation processes.[5]

The elimination mechanism of sulfinyl-PPV precursor polymers is considered to take place via a syn-elimination (via a five-membered ring) in which the intermediate has a planar structure. This planar conformation can, in general, account for the selectivity to form trans double bonds because steric hindrance between phenyl groups obstructs the formation of a cis double bond (Scheme 1, **I**). This process leads to the expulsion of sulfenic acids as the vinylic bond is formed.[6−8] The sulfenic acids are unstable and dimerize to give thiosulfinates with concomitant loss of water.[9] The thiosulfinates disproportionate with the formation of thiosulfonates and disulfides (Scheme 1, **II**).[10−12] These products are called elimination products in this study.

The conjugated polymer in this study is poly[2-(3′,7′-dimethyloctyloxy)-5-methoxy-1,4-phenylenevinylene] or OC_1C_{10}-PPV. OC_1C_{10}-PPV is soluble in its conjugated form due to the alkoxy chains (OC_{10} and OC_1) on the polymer backbone (Figure 1).[13−16] These materials have gained a lot of interest in the literature because of their relatively easy synthesis, their good processing capabilities into single-layer devices, and their high luminescence yields.[17] Recently, promising results were also obtained for photovoltaic (solar) cells.[18−21] Therefore, OC_1C_{10}-PPV has become a standard electroluminescent material inside the polymeric LED (PLED) and plastic solar cell research. An

[†] Universiteit Hasselt.
[‡] Vrije Universiteit Brussel.
[§] IMEC.
* Corresponding author: e-mail bvmele@vub.ac.be; phone +32-2-6293276 or 3288; Fax 32-2-6293278.

10.1021/ma051727g CCC: $33.50
Published on Web 03/30/2006

Scheme 1. Conversion Process of Sulfinyl-PPV Precursor Polymer to the Conjugated PPV Polymer: (I) Mechanism of the Elimination Reaction; (II) Dimerization and Disproportionation of Sulfenic Acids

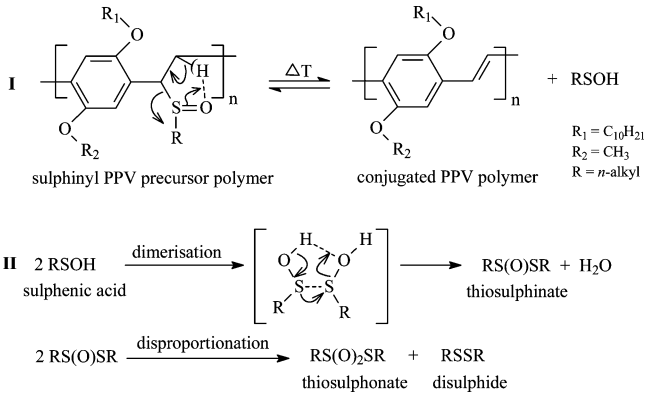

important disadvantage of these materials, however, is that in some cases it is difficult to develop the multilayer structures required for highly efficient LEDs since cosolubility of the different materials is hard to avoid.

The most used synthetic route to prepare the OC_1C_{10}-PPV conjugated polymer is the direct "Gilch route", a one-step synthesis in basic environment.[22] Another promising synthetic route developed by Vanderzande and co-workers, the "sulfinyl route", is a nonionic precursor route.[23−26] Note that since the OC_1C_{10}-PPV conjugated polymer is a soluble PPV derivative, the thermal elimination from a precursor polymer to the conjugated form can also be carried out in solution. This is important for applications where an already conjugated polymer can be deposited on the substrate, instead of a precursor polymer film that has to be eliminated on the substrate itself (such as PPV). A huge advantage of performing this elimination in solution is that the elimination products of the disproportionation reaction of thiosulfinate do not interfere with the conjugated polymer, in contrast with elimination from a polymer film (solid state). Nevertheless, solid-state elimination from a precursor polymer film may be desirable in those applications where the deposition of conjugated PPV is impossible. In such a case, the precursor polymer film can be deposited from other solvents (avoiding cosolubility), and even precursors of nonsoluble variants of the PPV's could be used.

Modulated temperature differential scanning calorimetry (MTDSC) is very useful in studying phase transitions in polymeric systems [27]and will be used to determine the interaction between the conjugated polymer and the solvent. Recently, phase separation between polymer−polymer and polymer−solvent systems has been studied using the heat capacity signal from MTDSC.[28−30] In this work, two different solvents will be studied: chlorobenzene and toluene. Both solvents are used because of their high boiling points: 130 and 111 °C, respectively. Chlorobenzene is a good solvent for spin-coating, but it is less suitable on a large scale because of health risks, while toluene is more used in industry.

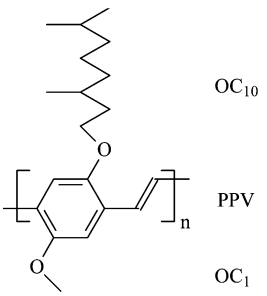

Figure 1. Structure of poly[2-(3′,7′-dimethyloctyloxy)-5-methoxy-1,4-phenylenevinylene (OC_1C_{10}-PPV).

In this paper, information from FT-IR spectroscopy, UV−vis spectroscopy, and MTDSC as in-situ analytical techniques will be combined to develop a clear picture of the conversion process in the solid state and in solution. It is a challenge to combine these data to one global picture.

Experimental Part

Thermal Analytical Techniques and Sample Preparation. The in-situ FT-IR elimination reactions in the solid state were performed in a Harrick high-temperature cell (Safir), which is positioned in the beam of a Perkin-Elmer spectrum one FT-IR spectrometer (nominal resolution 4 cm^{-1}, summation of 16 scans). The temperature of the sample is controlled by a Watlow (serial number 999, dual channel) temperature controller. The precursor polymer was spin-coated from a $CHCl_3$ solution (6 mg/mL) on a KBr pellet at 500 rpm. First the small heating cell is preheated to the desired temperatures (60, 65, 70, 75, and 80 °C). Afterward, the spin-coated KBr-pellet is brought into the preheated cell, which is continuously flushed with nitrogen (open system). The spin-coated KBr pellet (diameter 25 mm, thickness 1 mm) is in direct contact with the heating element. "Timebase software" (Perkin-Elmer) is used to follow the processes.

In-situ UV−vis measurements in the solid state were performed on a Cary 500 UV−vis−NIR spectrophotometer, adapted to contain a Harrick high-temperature cell (scan rate 600 nm/min, continuous run from 200 to 600 nm). The precursor polymers were spin-coated from a $CHCl_3$ solution (6 mg/mL) on a quartz glass (diameter 25 mm, thickness 3 mm) at 700 rpm. The quartz glass was heated in a Harrick high-temperature cell and positioned in the beam of the UV−vis−NIR spectrophotometer. Spectra were taken continuously. The experiments are performed in the same manner as the in-situ FT-IR measurements. All measurements were performed under a continuous flow of nitrogen (open system). "Scanning Kinetics software" (Varian) is used to follow the processes.

For the in-situ UV−vis measurements in solution, a solution with a concentration of 8.33×10^{-5} g/mL is brought in a quartz cuvette (closed system) and is then positioned in a cuvette heating accessory (Perkin-Elmer) that can be placed in the beam of the UV−vis spectrophotometer (Perkin-Elmer Lambda 45 UV−vis). The temperature of the heating accessory is controlled with a heating circulator (Julabo HD-4, Julabo Labortechnik GmbH). Isothermal experiments were performed at 70, 75, 80, 85, 90, and 100 °C.

The modulated temperature differential scanning calorimetry (MTDSC) measurements were performed on a TA Instruments modulated 2920 DSC with MDSC option and equipped with a refrigerated cooling system. Helium was used as a purge gas (25 mL min^{-1}). Indium and cyclohexane were used for temperature calibration; the former was also used for enthalpy calibration. Heat capacity calibration was performed with a poly(methyl methacrylate) standard (PMMA) supplied by Acros.[31] The heat capacity difference between 150 and 80 °C is used, one temperature above and one temperature below the glass transition temperature (T_g) of PMMA, to make sure that heat capacity changes were adequately measured. The measured difference in heat capacity before and after the T_g of PMMA (ΔC_p, measured) is compared with the corresponding literature value (ΔC_p, literature) to calculate the calibration factor K_{C_p}. It is necessary to calibrate the instrument every time a new type of pan or a new modulation period is used. The isothermal experiments in the solid state are performed in aluminum Perkin-Elmer (PE) 10 μL−0.15 mm pans. A temperature modulation of ±0.5 °C (amplitude) per 60 s (period) is used (noted as 0.5 °C/60 s). The sample weight is between 5 and 10 mg. For the solid-state MTDSC experiments, films of either the precursor polymer or the conjugated polymer are pressed at 35 °C to a thickness of 500 μm between an aluminum foil. Reproducible MTDSC measurements were obtained using this method of sample preparation. The experiments in solution are carried out in PE 40 μL−0.15 mm pans

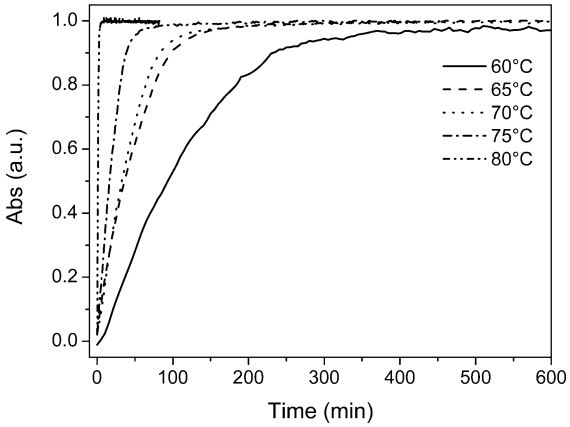

Figure 2. Evolution of the absorbance of the trans double bond at 965 cm^{-1} vs time for the elimination of *n*-octylsulfinyl OC_1C_{10}-PPV at 60, 65, 70, 75, and 80 °C.

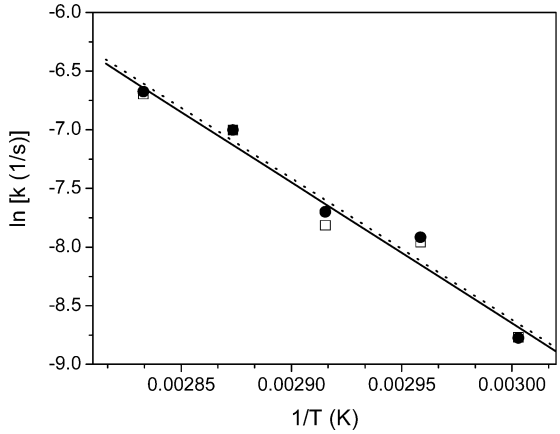

Figure 3. Arrhenius plot for the elimination reaction of *n*-octylsulfinyl OC_1C_{10}-PPV obtained with in-situ FT-IR spectroscopy in solid state: (□, —) appearance of trans-vinylene bond at 965 cm^{-1}; (●, – – –) disappearance of sulfinyl group at 1046 cm^{-1}. Lines are linear regression results.

and in high-pressure stainless steel (HPS) pans. The HPS pans are used in experiments where temperatures above 100 °C are applied (nonisothermal experiments). Modulation conditions of ±0.5 °C/100 s are selected for the heavier HPS pans. For the experiments in solution, a mixture of about 50% (m/m) is prepared directly in the pan by adding an equal mass of a given solvent to a weighed amount of the precursor polymer. Each pan is hermetically sealed to avoid weight losses of elimination products (closed system) and is weighed before and after the MTDSC experiment to check for weight losses.

Molar masses and molar mass distributions were determined relative to polystyrene standards with a narrow polydispersity (Polymer Labs) by size exclusion chromatography (SEC). Separation to hydrodynamic volume was obtained using a Spectra series P100 (Spectra Physics) equipped with a precolumn (5 μm, 50 mm × 7.5 mm, guard, Polymer Labs) and two mixed-B columns (10 μm, 2 × 300 mm × 7.5 mm, Polymer Labs) and a refractive index detector (Shodex) at 40 °C. SEC samples are filtered through a 0.45 μm filter. HPLC grade tetrahydrofuran (p.a.) is used as the eluent at a constant flow rate of 1.0 mL/min. Toluene is used as flow rate marker.

^{1}H NMR spectra were obtained in $CDCl_3$ at 300 MHz on a Varian Inova spectrometer using a 5 mm probe. Chemical shifts (δ) in ppm were determined relative to the residual $CHCl_3$ resonance shift (7.24 ppm). The ^{13}C NMR experiments were recorded at 75 MHz on the same spectrometer using a 5 mm broadband probe. Chemical shifts were defined relative to the ^{13}C resonance shift of $CHCl_3$ (77.0 ppm).

Materials. The synthesis and characterization of the *n*-alkylsulfinyl OC_1C_{10}-PPV precursor polymers and the OC_1C_{10}-PPV conjugated polymer are described in the literature.[32,33]

Results and Discussion

1. Solid-State Conversion Process of Alkylsulfinyl OC_1C_{10}-PPV Precursor Polymers. 1.1. Kinetic Analysis of the Elimination Reaction in Isothermal Conditions, Studied with in-Situ FT-IR Spectroscopy. To determine the rate of conversion of the precursor polymer into the conjugated material at a certain temperature, the disappearance of the sulfinyl group at 1046 cm^{-1} (consumption of precursor) and the formation of the trans-vinylene double bond at 965 cm^{-1} (production of conjugated polymer) were measured. The evolution of the latter vs time is plotted in Figure 2 at several temperatures for *n*-octylsulfinyl OC_1C_{10}-PPV.

All curves in Figure 2 follow first-order kinetics of the elimination reaction. From the calculated first-order rate constants (k) at each temperature, the activation energy (E_A) of the elimination reaction was determined according to an Arrhenius law ($\ln k = \ln A - E_A/RT$; depicted in Figure 3).

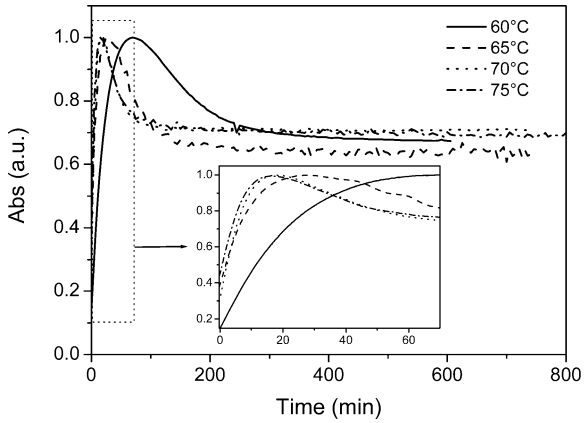

Figure 4. Evolution of the absorbance of λ_{max} at 376 nm vs time for the elimination of *n*-octylsulfinyl OC_1C_{10}-PPV at 60, 65, 70, and 75 °C. The inset is an expansion of the region indicated by the dotted box.

The activation energy (E_A) calculated from the disappearance of the precursor polymer (sulfinyl group at 1046 cm^{-1}) is 100 ± 10 kJ/mol. E_A for the formation of the conjugated OC_1C_{10}-PPV polymer (trans-vinylene double bond at 965 cm^{-1}) is 100 ± 11 kJ/mol. From theoretical modeling for the elimination reaction to 2,2′,5,5′-tetramethoxystilbene,[34] a value for E_A of 100.9 kJ/mol is obtained, which is in good agreement with these FT-IR results.[35] The first-order rate constant at 70 °C is about 5.0×10^{-4} s^{-1}.

1.2. Kinetic Analysis of the Elimination Reaction in Isothermal Conditions, Studied with in-Situ UV−Vis Spectroscopy. By plotting the UV−vis absorbance at 490 nm (λ_{max} of the conjugated OC_1C_{10}-PPV polymer) as a function of time, the formation of the larger conjugated segments can be determined.[36] Since these are not immediately formed upon elimination, an analysis of the temperature dependence of these plots yields an "apparent" activation energy. To obtain the activation energy of the elimination reaction, the formation of smaller conjugated segments (dimers) should be determined. Therefore, λ_{max} at 376 nm is plotted as a function of time at different temperatures in Figure 4. At the start of the elimination there is an increase in the absorbance at 376 nm, but as soon as the elimination reaction progresses, longer conjugated segments are formed at the expense of the shorter ones, corresponding to a decrease in the absorbance at 376 nm.

The increase in the absorbance at 376 nm follows first-order kinetics at the different temperatures (inset of Figure 4). From these data, the activation energy for the conversion reaction can be calculated to be 92 kJ/mol. This value is consistent with the E_A values obtained from the in-situ FT-IR measurements in the solid state (see section 1.1). It should be emphasized that the FT-IR results more specifically focus on the earliest stages of the conversion process, when stabilization of the transition state by long-range π-conjugation and electronic correlation is most limited. An explanation for the apparent decrease of the energy barrier in the UV−vis measurements is the rather significant influence of temperature on the width of bands in the UV−vis spectra of OPV segments.[37,38] As the UV−vis absorbance at one specific wavelength was used here, the enhancement of the amplitude of molecular motions (rotations, vibrations, etc.) with increasing temperatures will also contribute to an apparent decrease of the energy barrier. As the repeat unit normalized extinction coefficient remains roughly constant, one could fully integrate the signal pertaining to the lowest $\pi-\pi^*$ transition to estimate the extent of elimination.[39] This approach was not used here, as comparison to the absorbance at a specific wavelength corresponding to the formation of smaller conjugated segments (376 nm) was preferred for comparison with the FTIR results.

1.3. Study of the Elimination Reaction in Isothermal Conditions with MTDSC. One of the important reasons for selecting isothermal experiments is the possibility of separating the different reactions of the elimination process (Scheme 1). In general, when studying a reacting polymer system by means of MTDSC, the reaction enthalpy is detected in the nonreversing (NR) heat flow, while the reaction heat capacity (the change in heat capacity due to the chemical reaction, ΔC_p) can be inferred from the heat capacity signal.[40] When the conversion process is studied isothermally in MTDSC (Figure 5), an obvious change is seen in the specific heat capacity, ΔC_p, whereas no clear heat effect is observed in the NR heat flow (not shown). The same observations were made in nonisothermal MTDSC experiments, where this was interpreted as the effect of the immediate dimerization of the unstable sulfenic acid and the subsequent disproportionation reaction, giving rise to an overall thermoneutral reaction path. Therefore, ΔC_p was used to follow the conversion process in isothermal conditions. On the basis of nonisothermal experiments, it was decided to perform isothermal experiments at 70, 80, and 85 °C in an attempt to separate the dimerization from the disproportionation reaction. Also, higher temperatures (90 and 95 °C) were used, where the interference with the disproportionation reaction is more likely. Isothermal MTDSC measurements on the *n*-octyl- and *n*-butylsulfinyl OC_1C_{10}-PPV precursor polymers show little difference in the elimination behavior between the two R groups (Figure 5). The increase in ΔC_p in Figure 5 is due to the formation of the products in the dimerization and disproportionation steps. Because of the high specific heat capacity of water (4.19 J/(g K)), especially the formation of water during dimerization has a significant contribution to ΔC_p. For the *n*-octylsulfinyl OC_1C_{10}-PPV precursor at 70 °C, a continuous increase in the heat capacity is noticed until a plateau level is reached after 1400 min. A sigmoidal evolution in ΔC_p is seen in the initial stages of the conversion process (Figure 5, bottom). When the elimination temperature is raised, a faster increase in ΔC_p is seen with a maximum level after about 600, 300, 200, and 120 min at 80, 85, 90, and 95 °C, respectively.

An explanation for the sigmoidal evolution is the observation that the dimerization of sulfenic acid (liberation of water) and the disproportionation of thiosulfinate (liberation of thiosulfonate and disulfide) both contribute to ΔC_p. This can be confirmed by comparing the evolution in the formation of the trans-vinylene double bonds (absorbance at 965 cm^{-1}) as measured by FT-IR with the evolutions in ΔC_p. At 70 °C, for instance, ΔC_p only reaches a maximum level after 1400 min (Figure 5), while in the FT-IR experiment, the conjugated polymer reaches its maximum absorption (fully conjugated) already after 200 min (Figure 2). Thus, the formation of water and other products in the dimerization and disproportionation steps, visible as an increase in ΔC_p, is much slower than the formation of the conjugated system. The occurrence of the disproportionation reaction can be further confirmed by looking at the absorption peak corresponding to the formation of *n*-octylthiosulfonate (1130 cm^{-1}): at 80 °C, for example, this absorption peak is clearly present after an elimination time of 1100 min. Thus, it is difficult to separate the consecutive elimination and disproportionation reactions at elimination temperatures above 70 °C.

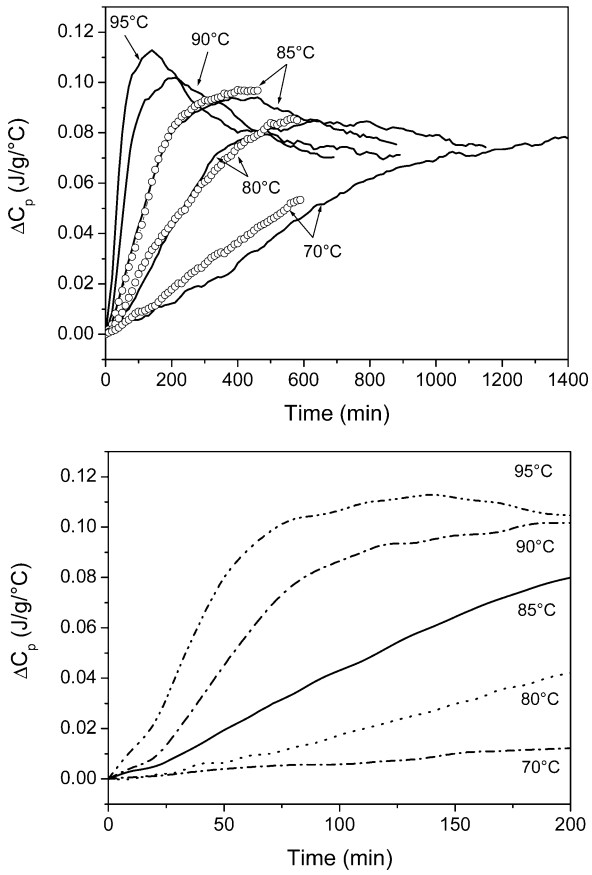

Figure 5. Heat capacity change ΔC_p vs time from isothermal MTDSC experiments on *n*-octylsulfinyl OC_1C_{10}-PPV precursor polymer at 70, 80, 85, 90, and 95 °C (top and bottom, lines) and comparison with *n*-butylsulfinyl OC_1C_{10}-PPV precursor polymer at 70, 80, and 85 °C (top, ○).

To explain the decrease in ΔC_p in the final stages of the conversion process, gel permeation chromatography (GPC) measurements were performed on each sample, following the isothermal MTDSC experiments of Figure 5. The molar masses (M_w) and polydispersities (D) are summarized in Table 1. M_w and D of a conjugated OC_1C_{10}-PPV polymer eliminated in solution (without elimination products) is ca. 390 000 g/mol and 2.7, respectively.

From these GPC results, it is clear that M_w and D increase with increasing temperature. We have also repeated the isothermal experiment at 95 °C with an isothermal period of only 50 min (just before reaching the maximum in the change of C_p) and 120 min (at the maximum in ΔC_p). At 95 °C, M_w and

Table 1. Molar Mass (M_w) and Polydispersity (D) after Isothermal MTDSC Experiments on *n*-Octylsulfinyl OC_1C_{10}-PPV Precursor Polymer in Solid State (Experiments Shown in Figure 5)

experiment temperature−time	M_w (g/mol)	D
70 °C−1700 min	408 000	3.5
80 °C−1100 min	573 000	4.1
85 °C−1200 min	662 000	4.7
90 °C−900 min	965 000	5.9
95 °C−50 min (before max)	325 000	2.5
95 °C−120 min (at max)	744 000	2.9
95 °C−600 min (after max)	841 000[a]	7.1

[a] Highest molecular fractions are withheld by the filter.

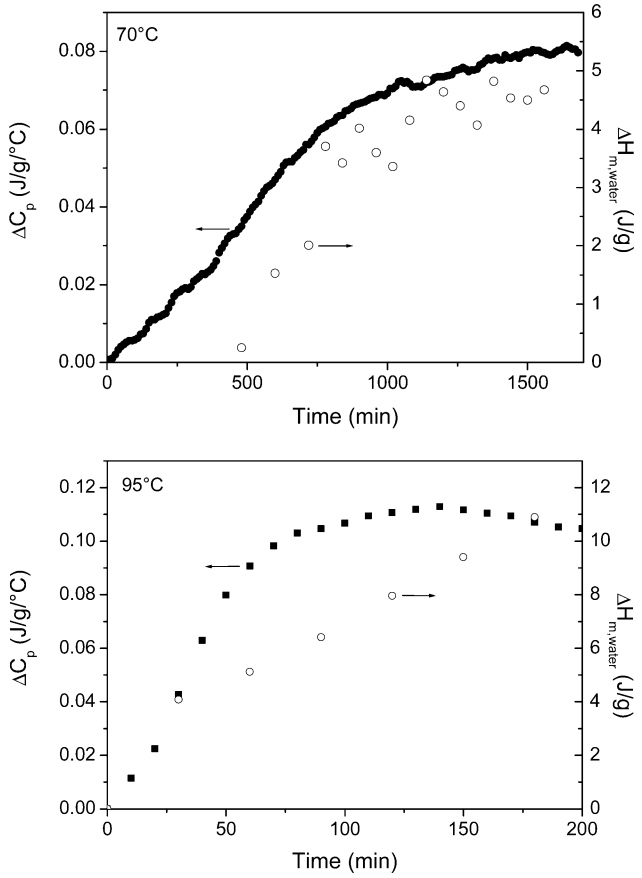

Figure 6. Heat capacity change ΔC_p and melting enthalpy of water vs time from MTDSC experiments on *n*-octylsulfinyl OC_1C_{10}-PPV precursor polymer at 70 °C (top) and 95 °C (bottom).

D increase with longer isothermal periods. It is therefore likely that cross-linking of the conjugated polymer occurs during the conversion process, caused by the elimination products that are liberated during the isothermal elimination reactions, and starting around the maximum in ΔC_p. Indeed, while the conjugated polymer is still soluble before the maximum of ΔC_p at 95 °C, it is insoluble after the maximum of ΔC_p at 95 °C. Thus, the decrease after the initial increase in ΔC_p (Figure 5) is probably related to network formation and seems to occur for all elimination experiments above 70 °C.

In Figure 6, ΔC_p (from Figure 5) and the melting enthalpy of water ($\Delta H_{m,water}$) are plotted as a function of elimination time at temperatures of 70 and 95 °C. $\Delta H_{m,water}$ is calculated from the melting peak around 0 °C, as obtained from the total heat flow in nonisothermal MTDSC experiments after different elimination times at these temperatures. Since $\Delta H_{m,water}$ only indicates the amount of water that is liberated during the conversion process, while ΔC_p also contains a contribution of the disproportionation reaction, both evolutions hold complementary information. At 70 °C, no melting peak is visible at the beginning of the conversion process ($\Delta H_{m,water} = 0$ J/g for times of 0 up to 400 min). This probably means that water, which is first liberated in the dimerization reaction, interacts with the main chain via the alkoxy chains (H-bonding). From 400 min on, the melting peak of water becomes visible and both curves (ΔC_p and $\Delta H_{m,water}$) similarly increase. Since no additional effect is seen in ΔC_p, the disproportionation reaction does not seem to occur at 70 °C. At 95 °C, the melting of water can be detected from the beginning of the conversion process. As $\Delta H_{m,water}$ increases almost linearly (after 30 min), while the increase in ΔC_p first slows down (near 60 min) and then changes to a decrease (near 140 min), the disproportionation reaction seems to take place at this temperature.

Table 2. Percentages of Water Liberated in the Dimerization Process during the Conversion Process of *n*-Octylsulfinyl OC_1C_{10}-PPV Precursor Polymer in Solid State, Calculated from the Melting Peak of Water at around 0 °C in the Heat Flow Signal (MTDSC)

R group	experiment	heat of melting (J/g)	% water calcd from heat of melting	peak temp (°C)	C_p increase (J/(g K))
n-butyl	70 °C−600 min	0.487	0.15	−22/−7.1	0.056
	80 °C−600 min	4.253	1.27	−22/−7.1	0.095
	85 °C−600 min	6.384	1.92	−2.84	0.110
n-octyl	70 °C−600 min	1.074	0.32	−3.14	0.051
	70 °C−1700 min	4.743	1.42	−3.13	0.083
	80 °C−600 min	5.351	1.6	−2.26	0.087
	80 °C−1100 min	6.035	1.81	−1.9	0.103
	85 °C−600 min	6.718	2.01	−3.14	0.090
	85 °C−900 min	7.376	2.21	−1.81	0.100
	90 °C−900 min	7.935	2.38	−2.69	
	95 °C−600 min	7.725	2.31	−3.66	

Table 3. Theoretical Weight Fractions of Products Formed during the Conversion Process of *n*-Alkylsulfinyl OC_1C_{10}-PPV Precursor Polymer in Solid State

	sulfenic acid	thiosulfinate	water
n-butyl	312 g/mol	194 g/mol	18 g/mol
	27%*	24.7%	2.3%
n-octyl	162 g/mol	306 g/mol	18 g/mol
	36%*	34%	2%

To quantify the amount of water formed during the conversion process, the melting enthalpies of water ($\Delta H_{m,water}$, Figure 6) can be compared to the literature value for the melting enthalpy of water (equal to 6.01 kJ/mol or 333.9 J/g[41]). The resulting percentages of water formed as a function of the temperature and time of elimination and the type of R-group (defined in Scheme 1) are shown in Table 2. The theoretical maximum percentage of water formed during the conversion process can be calculated using the reaction equation of the dimerization reaction, as shown in Table 3. When the calculated percentages are compared to the experimental ones, it can be noticed that for the *n*-octylsulfinyl OC_1C_{10}-PPV precursor polymer the theoretical maximum percentage of water (2%) is reached at the end of the conversion process at elimination temperatures from 85 to 95 °C. For experiments at 80 and 70 °C, only 1.8% and 1.4% water are obtained, respectively, after long elimination times (1100 and 1700 min, respectively). Thus, for these lower temperatures the dimerization reactions do not attain completion.

Table 2 also indicates the change in heat capacity for the different time−temperature conditions. From the specific heat capacity of water at a pressure of 1 bar (4.2 J/(g K)), the theoretical maximum increase in ΔC_p resulting from the formation of water can be calculated using the maximum attainable water contents (Table 3), giving 0.097 and 0.084 J/(g K) for the *n*-butylsulfinyl and *n*-octylsulfinyl OC_1C_{10}-PPV polymers, respectively. The higher experimental values of ΔC_p

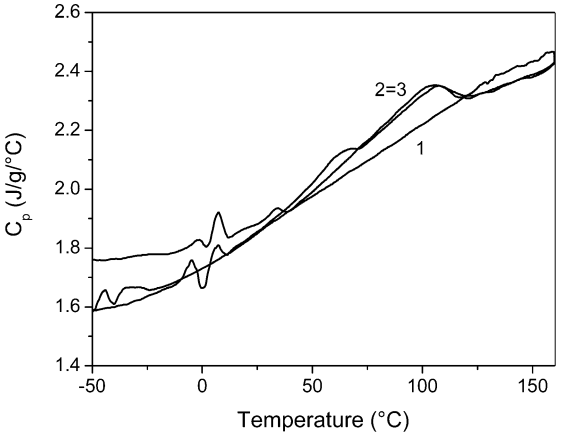

Figure 7. Heat capacity C_p vs temperature from a nonisothermal measurement on the *n*-octylsulfinyl OC_1C_{10}-PPV precursor polymer in toluene (43% (m/m)). The sample is heated from −50 °C up to 200 °C at 2.5 °C/min (1), followed by a cooling (2) and a second heating (3).

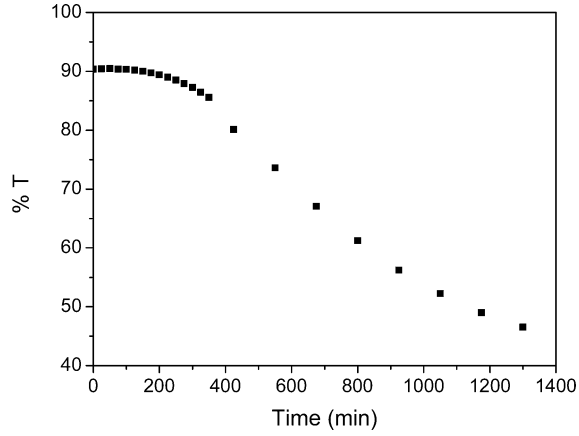

Figure 8. Transmission (%) at 580 nm as a function of time at 80 °C from in-situ UV−vis spectroscopy for a saturated mixture of *n*-octylsulfinyl OC_1C_{10}-PPV precursor polymer dissolved in toluene.

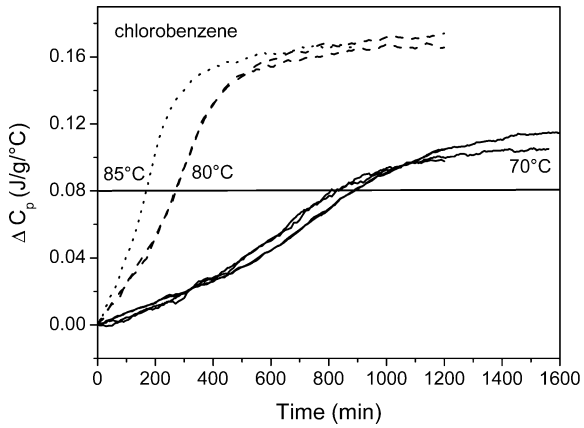

Figure 9. Heat capacity change ΔC_p vs time from isothermal MTDSC experiments at 70, 80, and 85 °C on 50% (m/m) mixtures of *n*-octylsulfinyl OC_1C_{10}-PPV precursor polymer in chlorobenzene. The reproducibility of the measurements at 70 and 80 °C is shown. The horizontal line indicates the final ΔC_p for the elimination in solid state.

for long elimination times (Table 2) indicate that not only water but also the other elimination products contribute to ΔC_p in these conditions, as concluded qualitatively before.

2. Liquid-State Conversion Process of *n*-Octylsulfinyl OC_1C_{10}-PPV Precursor Polymers. 2.1. Phase Separation As Induced by the Formation of the Conjugated Polymer. In Figure 7, a nonisothermal MTDSC experiment is shown which is carried out on a 43% (m/m) mixture of *n*-octylsulfinyl OC_1C_{10}-PPV precursor polymer in toluene. A broad peak is visible in the heat capacity signal in the cooling after the first heating. This could be an indication for phase separation between the polymer and the solvent, during which the composition of the coexisting phases changes continuously as a function of temperature.[30,42,43] In this case, the onset of this peak in the heat capacity upon cooling (around 110 °C) corresponds to the cloud point temperature. The second heating curve **(3)** has the same shape as the cooling curve **(2)**, revealing that remixing and demixing are reversible for this system. Performing such MTDSC heating−cooling experiments over a large concentration range would allow the construction of the phase diagram of the polymer−solvent system. We suppose an upper critical solution temperature behavior (UCST) for our polymer−solvent system.[42]

To confirm the occurrence of phase separation between the conjugated OC_1C_{10}-PPV polymer and toluene, a mixture (50% (m/m)) of conjugated polymer and toluene is prepared and heated until the polymer is dissolved and a transparent (red) solution is obtained. When this solution is cooled to ambient temperature, phase separation between the polymer and the solvent becomes visible. A red solution with some red polymer particles is obtained. By repeating this heating−cooling process, the reversibility of (re)mixing and demixing can be confirmed.

2.2. Study of the Elimination Reaction in Isothermal Conditions. To determine the activation energy E_A for the elimination reaction in solution with in-situ UV−vis spectroscopy, the absorbance at 367 nm was used in the same manner as before (section 1.2). A value of 80.8 kJ/mol is obtained for E_A, which is lower than the one from the solid-state UV−vis spectra (92 kJ/mol). The difference in E_A can be ascribed to an effect of the solvent on the mechanism of the elimination or to higher diffusion rates resulting from the lower viscosity. It has to be noted, however, that the procedure to determine E_A with UV−vis spectroscopy is less accurate than the procedure used in FT-IR spectroscopy, as from UV−vis experiments fewer data points are available in the beginning of the elimination reaction, because the shorter segments transform rapidly into longer conjugated segments upon elimination.

Moreover, the interference of phase separation with the UV−vis signal should not be overlooked. Phase separation in isothermal conditions is demonstrated by measuring the light transmittance with in-situ UV−vis spectroscopy. A saturated mixture of *n*-octylsulfinyl OC_1C_{10}-PPV precursor polymer is dissolved in toluene and heated to 80 °C, where it is held for 1300 min in the UV−vis spectrophotometer.

The end set of the absorption peak of the conjugated OC_1C_{10}-PPV polymer is around 550 nm. After longer periods at 80 °C, the end set of each UV−vis spectrum shifts to higher wavelengths due to light scattering from the particles that are formed. To demonstrate phase separation independently from the elimination reaction, the absorbance at 580 nm (>550 nm) is plotted as a function of time, shown in Figure 8. From this figure it is clear that phase separation sets in around 230 min at 80 °C.

The interference of phase separation in solution also complicates the analysis of the conversion process in isothermal conditions with MTDSC. Results for the elimination at different temperatures (70, 80, and 85 °C) of 50% (m/m) mixtures of *n*-octylsulfinyl OC_1C_{10}-PPV precursor polymer in toluene and chlorobenzene are shown in Figures 9 and 10, respectively. As concluded from the measurements in solid state (Figure 5), the

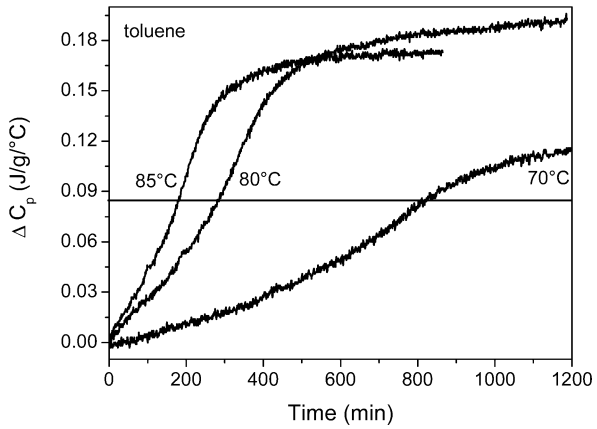

Figure 10. Heat capacity change ΔC_p vs time from isothermal MTDSC experiments at 70, 80, and 85 °C on 50% (m/m) mixtures of *n*-octylsulfinyl OC_1C_{10}-PPV precursor polymer in toluene. The horizontal line indicates the final ΔC_p for the elimination in solid state.

Table 4. Results Obtained Concerning the E_A (kJ/mol) of the Elimination Reaction of *n*-Octylsulfinyl Precursor Polymer with Different Spectroscopic Techniques in Solid State and in Solution

	solid state	solution
in-situ FT-IR	100	
in-situ UV−vis	92	81

increase in heat capacity is due to water and elimination products that are formed during the conversion process. It is important to note, however, that the increase in heat capacity is larger for the elimination in solution compared to the elimination in solid state (reference line in Figures 9 and 10). This confirms the occurrence of phase separation as previously pointed out using UV−vis spectroscopy. The fact that the changes in heat capacity with toluene are somewhat larger than with chlorobenzene could be indicative of the difference in solubility of OC_1C_{10}-PPV in these two solvents.

Conclusions

The conversion process from an *n*-octylsulfinyl OC_1C_{10}-PPV precursor polymer to the conjugated OC_1C_{10}-PPV polymer can be studied with several spectroscopic techniques. The formation of double bonds in the conjugated system can be followed using in-situ FT-IR spectrometry. In-situ UV−vis spectroscopy has the ability to detect the amount of conjugated segments formed during the elimination reaction. By performing the elimination at different temperatures, the activation energy of the elimination reaction can be determined, as summarized in Table 4.

The elimination process can also be studied using isothermal MTDSC experiments. In particular, the increase in the heat capacity corresponds to the formation of water (dimerization reaction) and other elimination products (disproportionation reaction). At temperatures above 70 °C (∼90 °C), the dimerization reaction and disproportionation reaction occur simultaneously. At 70 °C or lower only water is formed. Prolonged presence of elimination products during the conversion reaction leads to side reactions, such as cross-linking, which may jeopardize the structural integrity of the conjugated system and thus must be avoided. By calculating the melting heat of water from the nonreversing heat flow in nonisothermal posttreatment experiments, an independent probe for water formation can be obtained. In the future, the combination of the different in-situ techniques should allow for further quantification of the reaction kinetics and the reaction mechanism of the conversion process. When the elimination is performed in solution, MTDSC, and especially the heat capacity signal, not only provides information about the formation of elimination products but also enables one to detect the occurrence of phase separation during the conversion process. In the nonisothermal experiments, a small baseline shift is visible in the heat capacity signal at high temperature, which is an indication for phase separation. In the isothermal experiments, the increase in heat capacity is larger for the elimination in solution compared to the elimination in solid state, which is also an indication not only that the increase in heat capacity is due to the elimination process itself but also that phase separation interferes beyond a certain conversion.

Acknowledgment. The Institute for the Promotion of Innovation by Science and Technology in Flanders (IWT) is acknowledged for the PhD grant for E. Kesters. The Inter University Attraction Pole (IUAP) supported by the Belgian Government and the Research Foundation−Flanders (FWO−Vlaanderen) and BOF−UHasselt are acknowledged for financial support. The work of S. Swier was supported by grants of the IWT. G. Van Assche is Postdoctoral Fellow of the Research Foundation−Flanders (FWO−Vlaanderen).

References and Notes

(1) Wessling, R. A. *J. Polym. Sci., Polym. Symp.* **1985**, *72*, 55.
(2) Louwet, F. Ph.D. Thesis, Limburgs Universitair Centrum, Diepenbeek, Belgium, 1993.
(3) de Kok, M. Ph.D. Thesis, Limburgs Universitair Centrum, Diepenbeek, Belgium, 1999.
(4) de Kok, M. M.; van Breemen, A. J. J. M.; Carleer, R. A. A.; Adriaenssens, P. J.; Gelan, J. M.; Vanderzande, D. J. *Acta Polym.* **1999**, *50*, 28.
(5) Kesters, E.; Vanderzande, D.; Lutsen, L.; Penxten, H.; Carleer, R. *Macromolecules* **2005**, *38*, 1141.
(6) Kingsburry, C. A.; Cram, D. J. *J. Am. Chem. Soc.* **1960**, *82*, 1810.
(7) Shelton, J. R.; Davis, K. E. *Int. J. Sulfur Chem.* **1973**, *8*, 205.
(8) Yoshimura, T.; Tsukurimichi, E.; Iizuka, Y.; Mizuno, H.; Isaji, H.; Shimasaki, C. *Bull. Chem. Soc. Jpn.* **1989**, *62*, 1891.
(9) Trost, B. M.; Leung, K. K. *Tetrahedron Lett.* **1975**, *48*, 4197.
(10) Koch, P.; Ciuffarin, E.; Fava, A. *J. Am. Chem. Soc.* **1970**, *92*, 5971.
(11) Kice, J. L.; Cleveland, J. P. *J. Am. Chem. Soc.* **1973**, *95*, 109.
(12) Davis, F. A.; Jenkins, J. A.; Billmers, R. L. *J. Org. Chem.* **1986**, *51*, 1033.
(13) Braun, D.; Heeger, A. J. *Appl. Phys. Lett.* **1991**, *58*, 1982.
(14) Staring, E. G. J.; Demandt, R. C. J. E.; Braun, D.; Rikken, G. L. J.; Kessner, Y. A. R. R.; Venhuizen, T. H. J.; Wynberg, H.; ten Hoeve, W.; Spoelstra, K. J. *Adv. Mater.* **1994**, *6*, 934.
(15) Lee, J. K.; Schrock, R. R.; Baigent, D. R.; Friend, R. H. *Macromolecules* **1995**, *28*, 1966.
(16) Hilberer, A.; Brouwer, H. J.; van der Scheer, B. J.; Wildeman, J.; Hadziioannou, G. *Macromolecules* **1995**, *28*, 4525.
(17) Kim, S. T.; Hwang, D. H.; Li, X. C.; Grüner, J.; Friend, R. H.; Holmes, A. B.; Shim, H. K. *Adv. Mater.* **1996**, *8*, 979.
(18) Gerlinck, G. H.; Warman, J. M.; Staring, E. G. J. *J. Phys. Chem.* **1996**, *100*, 5485.
(19) Brabec, C. J.; Sariciftci, N. S.; Hummelen, J. C. *Adv. Funct. Mater.* **2001**, *11*, 15.
(20) van der Ent, L. *Kunststof Magazine*, April 3, 2001, 38.
(21) Munters, T.; Martens, T.; Goris, L.; Vrindts, V.; Manca, J.; Lutsen, L.; De Ceuninck, W.; Vanderzande, D.; De Schepper, L.; Gelan, J.; Saricifci, N. S.; Brabec, C. J. *Thin Solid Films* **2002**, *403*, 247.
(22) Gilch, H. G.; Wheelwright, W. L. *J. Polym. Sci., Part A: Polym. Chem.* **1966**, *4*, 1337.
(23) Louwet, F.; Vanderzande, D.; Gelan, J. *Synth. Met.* **1992**, *52*, 125.
(24) Louwet, F.; Vanderzande, D.; Gelan, J.; Mullens, J. *Macromolecules* **1995**, *28*, 1330.
(25) Louwet, F.; Vanderzande, D.; Gelan, J. *Synth. Met.* **1995**, *69*, 509.
(26) Issaris, A.; Vanderzande, D.; Gelan, J. *Polymer* **1995**, *38* (10), 2571.
(27) *Modulated-Temperature Differential Scanning Calorimetry: Theoretical and Practical Applications in Polymer Characterisation (Hot Topics in Thermal Analysis and Calorimetry)*; Reading, M., Hourston, D. J., Eds.; Springer: London, UK, 2006.
(28) Dreezen, G.; Groeninckx, G.; Swier, S.; Van Mele, B. *Polymer* **2001**, *42*, 378.
(29) Swier, S.; Pieters, R.; Van Mele, B. *Polymer* **2002**, *43*, 3611.
(30) Van der Heijden, P. L.; Mulder, M. H. V.; Wessling, M. *Thermochim. Acta* **2001**, *27*, 378.
(31) Gaur, U.; Wunderlich, B. *J. Phys. Chem. Ref. Data* **1982**, *11*, 313.

(32) van Breemen, A. Ph.D. Thesis, Limburgs Universitair Centrum, Diepenbeek, Belgium, 1999.
(33) Lutsen, L.; van Breemen, A. J.; Kreuder, W.; Vanderzande, D. J. M.; Gelan, J. M. J. V. *Helv. Chim. Acta* **2000**, *83*, 3113.
(34) Claes, L.; Francois, J.-P.; Deleuze, M. S. *J. Am. Chem. Soc.* **2002**, *124*, 7563.
(35) The value is the result of density functional theory calculations in a vacuum using a functional (MPW1K) especially designed for accurate calculations of energy barriers (ref 33 and references therein) and using a polarized basis set of triple-ζ quality (6-311G**). At this level, underestimations by ~10 kJ/mol are expected on these energy barriers, from a comparison with values derived from calculations at the confines of nonrelativistic quantum mechanics [CCSD(T)/cc-pVQZ level] on a smaller precursor.[34] Some care is recommended because the above calculations did not account for environmental (packing or solvent) effects and because enhanced π-conjugation in oligophenylenevinylene (OPV) segments larger than 2,2′,5,5′-tetramethoxystilbene is expected to yield a decrease of the activation energies for the internal conversion (Claes, L.; Francois, J. P.; Deleuze, M. S. Universiteit Hasselt, Belgium, personal communication).
(36) Kesters, E.; Lutsen, L.; Vanderzande, D.; Gelan, J.; Nguyen, T. P.; Molinié, P. *Thin Solid Films* **2002**, *403*−*404*, 120.
(37) Kwasniewski, S. P.; François, J.-P.; Deleuze, M. S. *Int. J. Quantum Chem.* **2001**, *85*, 557.
(38) Kwasniewski, S. P.; François, J.-P.; Deleuze, M. S. *J. Phys. Chem. A* **2003**, *107*, 5168.
(39) Padmanaban, G.; Nagesh, K.; Ramakrishnan, S. *J. Polym. Sci., Polym. Chem.* **2003**, *41*, 3929.
(40) Swier, S.; Van Mele, B. *J. Polym. Sci., Part B: Polym. Phys.* **2003**, *41*, 594.
(41) Lide, D. R. *Handbook of Chemistry and Physics*; CRC Press: Boca Raton, FL, 1998; pp 6.3−6.119.
(42) Arnauts, J.; De Cooman, R.; Vandeweerdt, P.; Koningsveld, R.; Berghmans, H. *Thermochim. Acta* **1994**, *1*, 238.
(43) Swier, S.; Van Durme, K.; Van Mele, B. *J. Polym. Sci., Part B: Polym. Phys.* **2003**, *41*, 1824.

MA051727G